environmental sciences proceedings

MDPI

Proceeding Paper

Analysis of Seismo-Ionospheric Irregularities Using the Available PRNs vTEC from the Closest Epicentral cGPS Stations for Large Earthquakes

Karan Nayak [1]*, Charbeth López Urias [1], Rosendo Romero Andrade [1], Gopal Sharma [2] and Manuel E. Trejo Soto [1]

[1] Faculty of Earth and Space Sciences, Autonomous University of Sinaloa, Mexico.
[2] North-Eastern Space Application Centre, Umiam, India
* Correspondence: karannayak203@gmail.com
† Presented at the 6th International Electronic Conference on Atmospheric Sciences, 2023

Abstract: The occurrence of earthquakes, which can strike suddenly without any warning, has always posed a potential threat to humanity. However, researchers worldwide have been diligently studying the mechanisms and patterns of these events in order to develop warning systems and improve detection methods. One of the most reliable indicators for predicting large earthquakes has been the examination of electron availability in the ionosphere. This study focuses on analyzing the behavior of the Total Electron Content (TEC) in the ionosphere during the 30-day period leading up to the three most devastating earthquakes of the past decade. Specifically, the data were examined from the cGPS stations closest to the epicenters: MERS for the Turkey earthquake with 7.8Mw on 02-06-2023, CHLM for the Nepal earthquake with 7.8Mw on 04-25-2015, and MIZU for the Japan earthquake with 9.1Mw on 03-11-2011. Notable positive and negative anomalies were observed for each earthquake, and the vertical Total Electron Content (vTEC) for each PRN (pseudo-random number) was plotted to determine the specific time of the TEC anomaly. The spatial distribution of vTEC for the anomalous specific time revealed that the anomalies were in close proximity to the earthquake epicenters, particularly within denser fault zones.

Keywords: Earthquake Precursors; LAIC; PRNs; vTEC

Citation: To be added by editorial staff during production.

Academic Editor: Firstname Lastname

Published: date

1. Introduction

Earthquakes, natural disasters that result from the sudden release of energy in the Earth's crust, have long been a subject of scientific study and fascination. Researchers have been exploring various methods to detect and predict earthquakes, including the analysis of earthquake precursors. Studies as such involved geological features [1,2], lineament analysis [3], latent heat increase [4], thermal anomalies [5], remote sensing, and multi-parametric approaches [6,7], have provided significant light for critical earthquake precursors. These precursors are subtle changes in the Earth's environment that occur before an earthquake and can provide valuable insights into the seismic activity.

The ionosphere, a layer of the Earth's atmosphere, is known to be affected by seismic activity. Large earthquakes can cause disturbances in the ionosphere that can be detected using GPS-derived vertical total electron content (vTEC). The detection of ionospheric TEC anomalies has been investigated in several studies using Global Ionospheric Maps (GIMs) and GPS-derived TEC data [8]. These studies have focused on analyzing TEC anomalies before major earthquakes, such as the Kumamoto-shi earthquake in Japan [8], the Alaska earthquake [9], and earthquakes in the Himalayan region [10]. By examining the TEC data from GPS stations located near the epicenter of these earthquakes, it is possible to identify significant anomalies in TEC values. The relationship between earthquakes and ionospheric TEC is a complex and ongoing area of research. Understanding these seismo-ionospheric irregularities can provide valuable insights into the mechanisms and processes associated with earthquakes. Furthermore, the detection of TEC anomalies could potentially contribute to the development of early warning systems for earthquakes.

In this research, we delved into the analysis of seismo-ionospheric irregularities using the available PRNs (Pseudo-Random Numbers) TEC data from the closest epicentral cGPS (continuous Global Positioning System) stations for three of the largest earthquakes in the last decade. We explored the methods used to detect and analyze TEC anomalies, the significance of these anomalies in earthquake precursor detection, and the potential applications of this research in improving our understanding of seismic activity.

2. Materials and Methods

The present study focused on the selected three most devastating and significant earthquakes occurring after 2010, each with a magnitude exceeding 7.5. To estimate Total Electron Content (TEC), close-range cGPS stations were employed, as detailed in Table 1. RINEX data from these stations, collected within a 45-day timeframe preceding each event, were scrutinized. Calculations utilized GPS-TEC software (version 3.2) developed by Gopi Krishna Seemala [11]. This software employed pseudo-range codes (P1 and P2) from GPS stations to compute Slant TEC (sTEC), which signifies the electron content between satellites and ionospheric receivers along a slant trajectory. This calculation involved a geometry-free linear combination of GPS observations [12].

Table 1. Earthquake and cGPS stations details used for TEC analysis.

Date	Mw	Location	Depth (Km)	cGPS	Dist. (Km)	Source
11-03-2011 (Japan)	9.1	38.297°N 142.373°E	29.0	MIZU	142	USGS
25-04-2015 (Nepal)	7.8	28.231°N 84.731°E	8.2	CHLM	57	USGS
06-02-2023 (Turkey)	7.8	37.226°N 37.014°E	10.0	MERS	256	USGS

The obtained sTEC values is then converted to vertical TEC (vTEC) while considering a model of the ionosphere resembling a thin spherical shell. In accordance with the single-layer model (SLM), an extremely thin layer positioned consistently above the Earth's surface was assumed to contain all the available free electrons [13]. The determination of vTEC at the ionospheric pierce point involved the utilization of a mapping function [14] based on the SLM. For this analysis, the ionospheric layer's altitude was fixed at 350 kilometers, and GPS receivers were sampled every 30 seconds.

A statistical foundation for the upper and lower boundary was established using a 15-day moving average and standard deviation, as illustrated by equation 1,

$$X \pm 1.34\sigma \quad (1)$$

where X signifies the mean and σ represents the standard deviation. Instances where vTEC values surpassed the upper and lower limits were classified as anomalies. For the anomaly days, the peak anomaly time for the positive and negative anomaly were deduced from equations 2 and 3,

$$PPA = TEC - UB \quad (2)$$

$$PNA = LB - TEC \quad (3)$$

where PPA is the Peak Positive Anomaly time, PNA is the Peak Negative Anomaly time, UB is the Upper Boundary and LB represents the Lower Boundary.

In addition to the TEC observations, the study also assessed Disturbance Storm Time (Dst) and Planetary Solar (KP) indices. A geomagnetic storm is identified when the Dst value crosses below -35 units, signifying a significant disturbance. To differentiate seismic anomalies from those observed on regular days without any impact from geomagnetic storms or solar flares, the study considered anomalies that occurred during periods of normal geomagnetic conditions.

3. Results and Discussions

The statistical analysis of ionospheric total electron content (TEC) is an important area of research for understanding the relationship between TEC and seismic activity. In the present research, we have investigated the correlations between TEC and pre-earthquake seismic activities to identify potential correlations between TEC anomalies and seismic activity for the Japan (9.1 Mw), Nepal (7.8Mw), and Turkey (7.8Mw) earthquakes.

3.1. Japan (9.1Mw) Earthquake

The Tohoku earthquake of Japan, also known as the Great East Japan earthquake, was a natural disaster that occurred on March 11, 2011. The earthquake was caused by thrust faulting at the plate boundary between the Pacific and North American plates. The earthquake had a magnitude of 9.1, making it the most powerful earthquake recorded in Japan since 1900 and the fourth most powerful ever detected worldwide. In Fig. 1, variations in Total Electron Content (TEC) are depicted for the period of 30 days prior to the earthquake of 11 March 2011, utilizing data from the closest continuous GPS (cGPS) station, MIZU, situated at 142 km from the earthquake's epicenter. The analysis reveals several positive anomalies between February 14-19 and March 3, 2011, as well as between March 7-10, 2011. The black and green polygon denotes instances where TEC values exceed the limits set by equation 1. Of notable significance, a pronounced anomaly displaying a TEC concentration exceeding 6 TECU was evident on March 8, 2011, markedly three days before the main earthquake event. The most substantial negative anomaly, dipping below 2 TECU, was observed on February 25, 2011. The PPA anomaly for 08 March is calculated to be 01.10 UTC while the NPA for 25 February is 05.47 UTC as per equations 2 and 3.

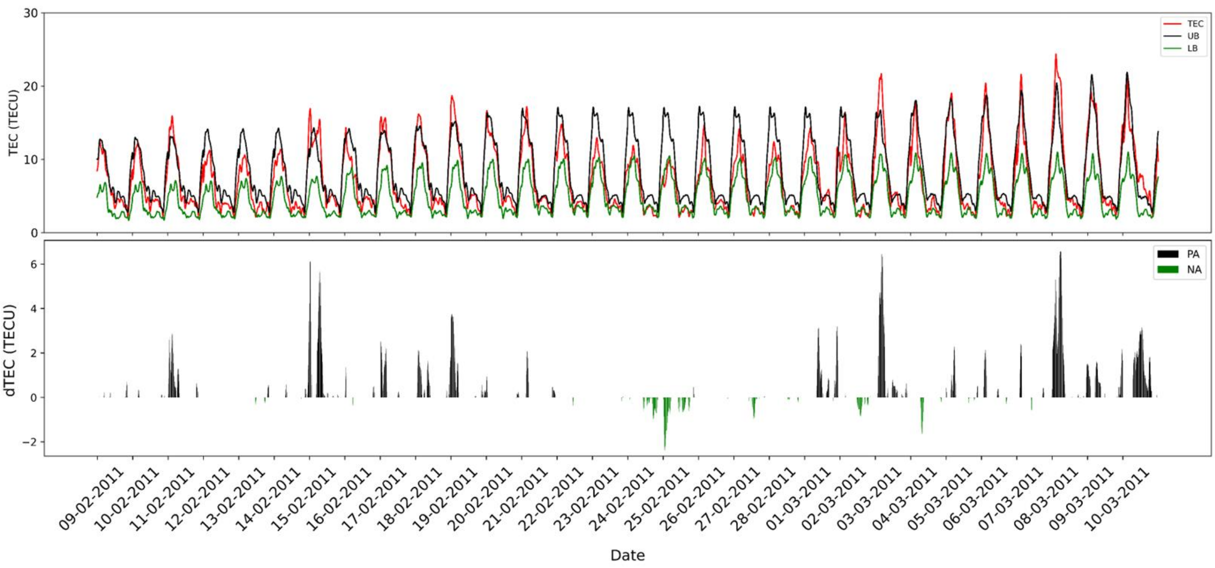

Figure 1. TEC variations prior to 30 days from the event, estimated from the nearest station MIZU.

Figure 2's upper-left and upper-right panels depict the PRNs available at the nearest station, MIZU, corresponding to the Peak Negative Anomaly (PNA) and Peak Positive Anomaly (PPA) times, respectively. The upper-left panel illustrates the vTEC behavior of each PRN at the anomaly time of 01:10 UTC during PNA. Conversely, the upper-right panel presents the vTEC behavior of each PRN at the PPA time of 05:47 UTC. The black line represents the anomaly time for each PNA and PPA. Applying kriging interpolation to the PRNs' vTEC values for each anomaly time produced the lower panel of Figure 2 for each anomaly time. The figure clearly illustrates that the anomaly zone lies in close proximity to the epicenter. Specifically, the PNA's most substantial negative anomaly occurred near the epicenter on February 25, 2011. In contrast, the positive anomaly is noted near the epicenter for PPA on March 8, 2011, as evidenced by the lower-right and lower-left panels of Figure 2.

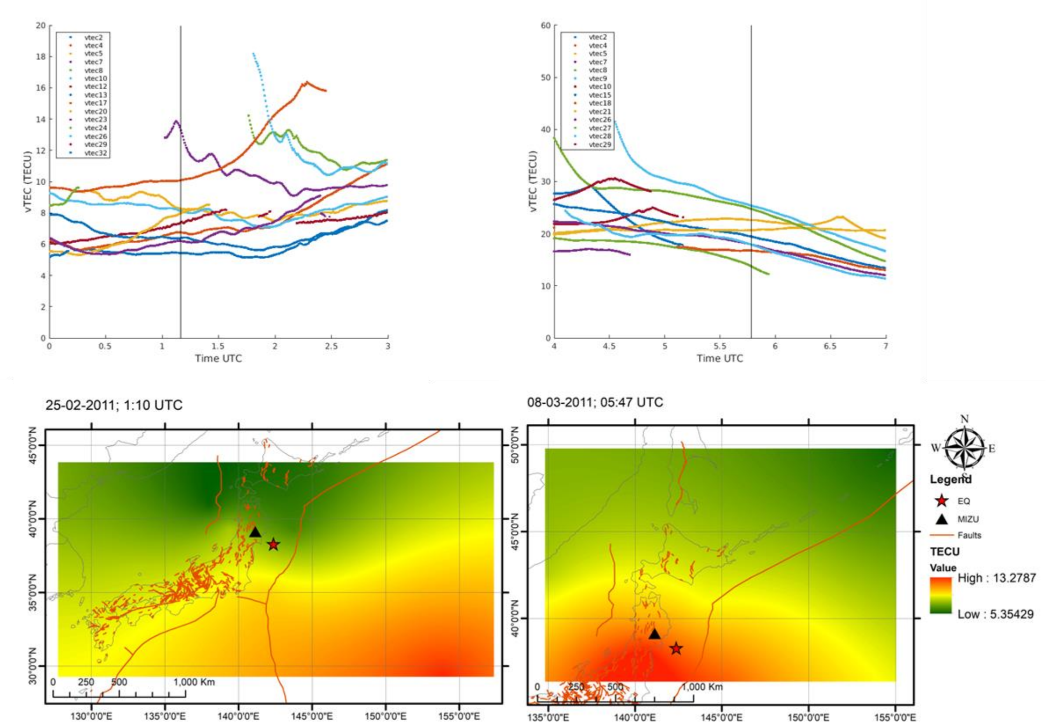

Figure 2. Behavior of available PRNs vTEC with respect to PNA (Upper left panel) and PPA (Upper right panel). Spatial interpolation of vTEC for PNA (Lower left panel) and PPA (Lower right panel). The red star is the epicentre and the black triangle represents the nearest cGPS.

3.2. Nepal (7.8Mw) Earthquake

The Nepal earthquake of April 25, 2015, also known as the Gorkha earthquake, was a devastating seismic event that struck Nepal with a magnitude of 7.8Mw. Figure 3 displays the TEC variations thirty days prior to the event. It is observed that a continuous positive anomaly is seen with the highest being on 25 April with a TECU difference of 25 units, just a few hours prior to the event. The PPA is calculated to be at 13.08 UTC, while a promiscuous negative anomaly was observed to be on 11 April with a TECU difference of 10 units, PNA calculated to be 07.45 UTC. Figure 4 illustrates the behavior of vTEC PRNs concerning both the Peak Negative Anomaly (PNA) and Peak Positive Anomaly (PPA). Consistent with the findings related to the Japan earthquake, it is also evident in this instance that the anomaly zone is situated in proximity to the epicenter. The upper-left and upper-right panels showcase the available PRN data at the nearest station, CHLM, for the PNA and PPA times, respectively. In the lower panel, it becomes clear that the most significant negative anomaly for the PNA occurred near the epicenter on April 11, 2015. Conversely, the positive anomaly was observed near the epicenter for PPA on April 25, 2015. These observations are clearly demonstrated in the lower-right and lower-left panels of Figure 4.

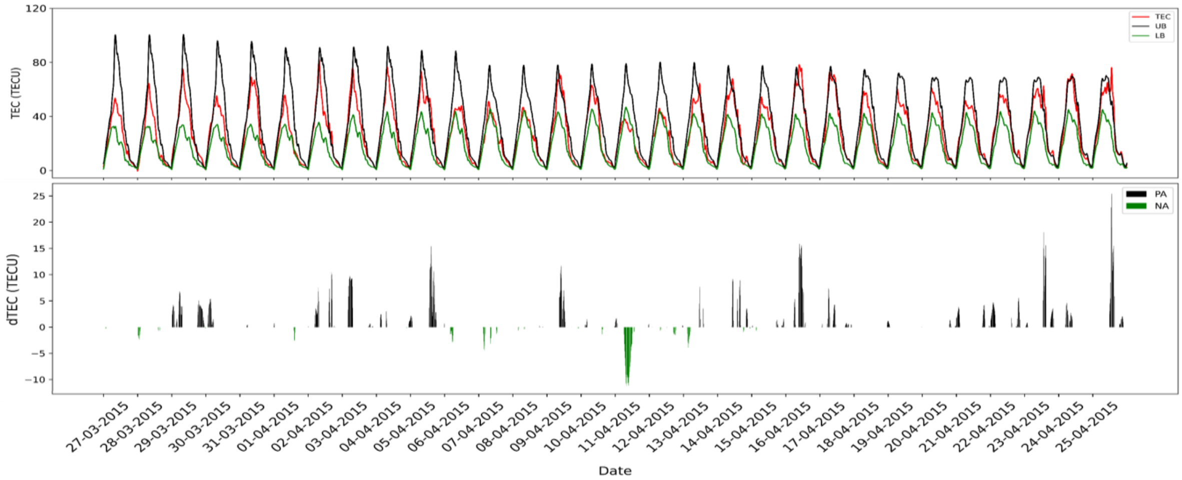

Figure 3. TEC variations prior to 30 days from the event, estimated from the nearest station CHLM.

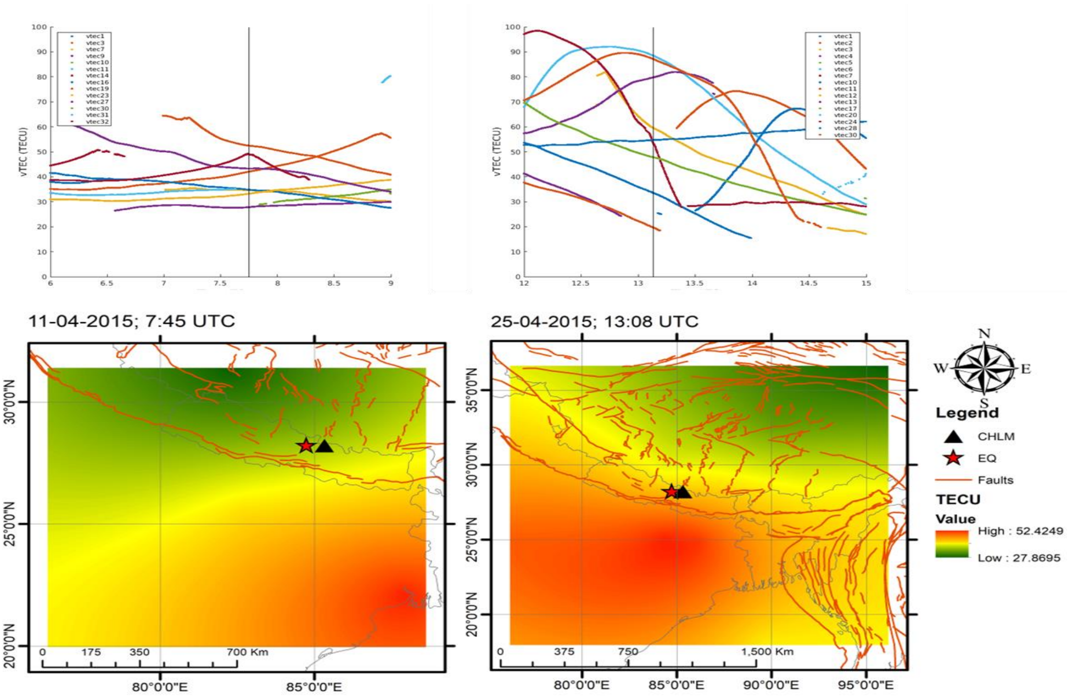

Figure 4. Behavior of available PRNs vTEC with respect to PNA (Upper left panel) and PPA (Upper right panel). Spatial interpolation of vTEC for PNA (Lower left panel) and PPA (Lower right panel). The red star is the epicentre and the black triangle represents the nearest cGPS.

3.3. Turkey (7.8Mw) Earthquake

The Turkey earthquake of February 6, 2023, was a major seismic event that struck southeastern Turkey near the Syrian border with a magnitude of 7.8Mw. On January 28, 2023, a highly notable positive anomaly in Total Electron Content (TEC) was observed, indicating a difference of 15 TECU, a full 8 days before an event. Interestingly, a negative anomaly characterized by a significant difference of 5 TECU was noticed just a day after the positive anomaly, as illustrated in Figure 5. The Peak Positive Anomaly (PPA) for

January 28 was determined to be at 10.16 UTC, while the Peak Negative Anomaly (PNA) for January 29 was calculated to be at 14.19 UTC. Similar to the conclusions drawn from the Japan and Nepal earthquakes, it is apparent in this case as well that the anomaly region is positioned close to the epicenter. As depicted in Figure 6, the upper-left and upper-right panels provide an overview of the PRN data available at the nearest station, MERS, for the PNA and PPA times, respectively. Notably, both the negative and positive anomalies at their respective peak times are situated in proximity to the epicenter. This emphasizes the notion that estimating TEC using PRNs from the nearest cGPS station could serve as an effective earthquake precursor.

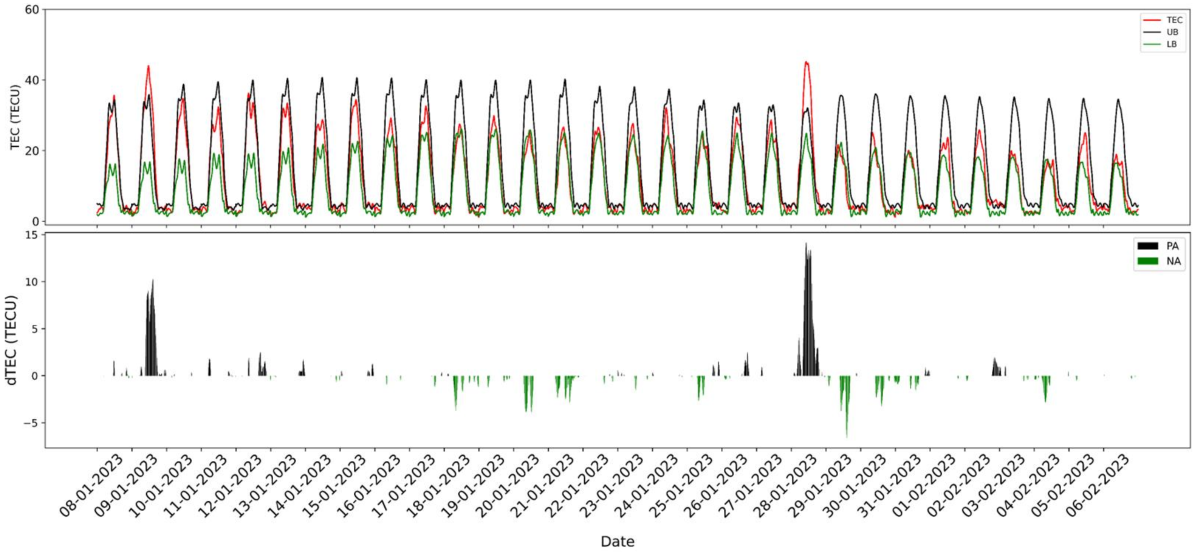

Figure 5. TEC variations prior to 30 days from the event, estimated from the nearest station MERS.

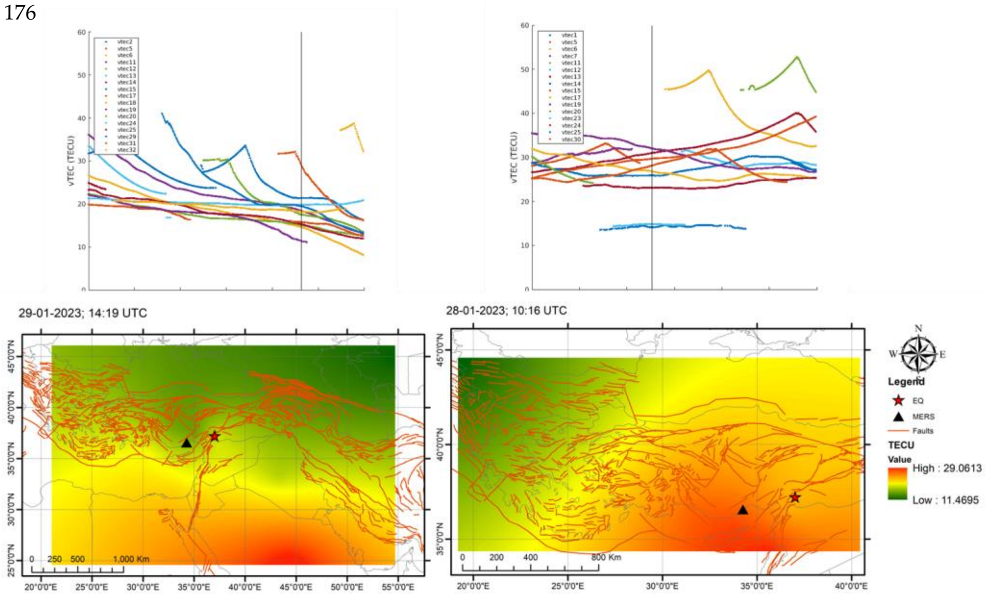

Figure 4. Behavior of available PRNs vTEC with respect to PNA (Upper left panel) and PPA (Upper right panel). Spatial interpolation of vTEC for PNA (Lower left panel) and PPA (Lower right panel). The red star is the epicentre and the black triangle represents the nearest cGPS.

4. Conclusions

In conclusion, this study's examination of ionospheric Total Electron Content (TEC) anomalies in relation to seismic activity reveals promising correlations for earthquake precursor detection. Analyzing notable earthquakes in Japan, Nepal, and Turkey, the research identifies consistent positive and negative TEC anomalies prior to seismic events, often near the epicenters. While preliminary, these findings suggest TEC anomalies could serve as indicators of impending earthquakes. Nevertheless, the study underscores the necessity of expanded datasets and further research to strengthen these connections. Ultimately, this work opens an avenue for advancing earthquake precursor detection methods and emphasizes the potential significance of TEC anomalies in seismic monitoring and early warning systems utilizing the available PRNs from the nearest cGPS stations.

Author Contributions: Conceptualization, K.N. and C.L.U.; methodology, K.N.; software, K.N.; validation, R.R.A., G.S., and M.T.S.; formal analysis, K.N.; investigation, K.N., and C.L.U.; resources, K.N.; data curation, C.L.U.; writing—original draft preparation, K.N.; writing—review and editing, K.N.; visualization R.R.A.; supervision, G.S.; project administration, M.T.S.; funding acquisition, K.N. All authors have read and agreed to the published version of the manuscript.

Funding: This work was carried out with the support (CVU: 1182470) of the National Council of Science and Technology (CONACyT) in Mexico.

Informed Consent Statement: Written informed consent has been obtained from the patient(s) to publish this paper

Acknowledgments: The authors would like to thank USGS, UNAVCO, National Oceanic and Atmospheric Administration (NOAA for freely providing high-quality data for the analysis.

Conflicts of Interest: The authors declare no conflict of interest

References

1. Malik, J. N., & Nakata, T. (2003). Active faults and related Late Quaternary deformation along the northwestern Himalayan Frontal Zone, India. Annals of Geophysics. http://hdl.handle.net/2122/996
2. Sharma, M. L., & Lindholm, C. (2012). Earthquake hazard assessment for Dehradun, Uttarakhand, India, including a characteristic earthquake recurrence model for the Himalaya Frontal Fault (HFF). Pure and Applied Geophysics, 169, 1601-1617. https://doi.org/10.1007/s00024-011-0427-7
3. Romero-Andrade, R., Trejo-Soto, M. E., Nayak, K., Hernández-Andrade, D., & Bojorquez-Pacheco, N. (2023). Lineament analysis as a seismic precursor: The El Mayor Cucapah earthquake of April 4, 2010 (MW7. 2), Baja California, Mexico. Geodesy and Geodynamics, 14(2), 121-129. https://doi.org/10.1016/j.geog.2022.08.001
4. Dey, S., & Singh, R. P. (2003). Surface latent heat flux as an earthquake precursor. Natural Hazards and Earth System Sciences, 3(6), 749-755. https://doi.org/10.5194/nhess-3-749-2003
5. Saraf, A. K., & Choudhury, S. (2005). Thermal remote sensing technique in the study of pre-earthquake thermal anomalies. J. Ind. Geophys. Union, 9(3), 197-207.
6. Hayakawa, M. (2009). Lower ionospheric perturbations associated with earthquakes, as detected by sub ionospheric VLF/LF radio signals. Electromagnetic Phenomena Associated with Earthquakes, edited by: Hayakawa M., Transworld Research Network, Trivandrum, India, 137-186.
7. Ouzounov, D., Liu, D., Chunli, K., Cervone, G., Kafatos, M., & Taylor, P. (2007). Outgoing long wave radiation variability from IR satellite data prior to major earthquakes. Tectonophysics, 431(1-4), 211-220. https://doi.org/10.1016/j.tecto.2006.05.042
8. Dong, Y.; Gao, C.; Long, F.; Yan, Y. Suspected Seismo-Ionospheric Anomalies before Three Major Earthquakes Detected by GIMs and GPS TEC of Permanent Stations. Remote Sens. 2022, 14, 20. https://doi.org/10.3390/rs14010020
9. Ruan Q, Yuan X, Liu H, Ge S. Study on co-seismic ionospheric disturbance of Alaska earthquake on July 29, 2021 based on GPS TEC. Sci Rep. 2023 Jul 1;13(1):10679. doi: 10.1038/s41598-023-37374-9.
10. Sharma, G., Mohanty, S., & Kannaujiya, S. (2017). Ionospheric TEC modelling for earthquakes precursors from GNSS data. Quaternary International, 462, 65-74. https://doi.org/10.1016/j.quaint.2017.05.007
11. Seemala, Gopi. (2012). GPS-TEC analysis software.
12. Y. Norsuzila, M. Abdullah, M. Ismail, Leveling process of total electron content (TEC) using Malaysian global positioning system (GPS) data, Am. J. Eng. Appl. Sci. 1 (2008).
13. U. Wild, Ionosphere and geodetic satellite systems: permanent GPS tracking data for modelling and monitoring, Geod.-Geophys. Arb. Schweiz. 48 (1994)
14. M.A. Sharifi, S. Farzaneh, Local ionospheric modeling using the localized global ionospheric map and terrestrial GPS, Acta Geophys. 64 (2016) 237e252.